tinued with either Boc-Gly, for peptide A9-Cdel, or with excess propionic anhydride:DIEA (1:1), for peptide G1-Ndel+A9-Cdel. Peptidyl resin was suspended in DCM, and 10 equivalents of isopropylamine was added followed by 1.2 equivalents of acetic acid (AcOH) [G. Ösapay, M. Bouvier, J. W. Taylor, in *Techniques in Protein Chemistry II*, J. J. Villafranca, Ed. (Academic Press, San Diego, 1991), pp. 221–231]. After shaking for 24 hours, resin was filtered and washed and filtrate was evaporated to a white material. This last cleavage-coupling step provided the desired COOH-terminal isopropylamino group (Cdel) (Table 1). Crude protected peptide (260 mg) was dissolved in TFA:DCM (50:50) (13 ml) and stirred at room temperature. After 1 hour, the mixture was evaporated and this chromatographically purified intermediate (22 mg) was dissolved in *n*-butanol:AcOH:water (1:1:1) (15 ml) and hydrogenated over 10% Pd on carbon (approximately 50 mg). After 20 hours, the mixture was filtered through Celite (Aldrich, Milwaukee, WI) and concentrated. We purified all crude peptides by reverse-phase chromatography (RP-HPLC) on a Vydac C_4 preparative column using linear gradients of acetonitrile in water (containing 20% isopropanol for peptides A9-Cdel and G1-Ndel+A9-Cdel). Purified peptides were characterized by amino acid analysis, FAB mass spectrometry, and analytical RP-HPLC. Stock solutions in dimethylsulfoxide were kept frozen.

22. D. N. Garboczi, D. T. Hung, D. C. Wiley, *Proc. Natl. Acad. Sci. U.S.A.* **89**, 3429 (1992). Gel filtration chromatography was done at room temperature with 20 mM tris-HCl (pH 7.5) containing 150 mM NaCl as eluent (0.8 ml/min) and with a Phenomenex Biosep Sec-S3000 column.
23. H.-C. Guo, M. Bouvier, D. C. Wiley, unpublished results.
24. M. L. Fahnestock, I. Tamir, L. Narhi, P. J. Bjorkman, *Science* **258**, 1658 (1992).
25. Circular dichroism experiments were done in 10 mM MOPS (pH 7.5), HLA-A2 complexes (0.18 mg/ml), and free β_2M (0.36 mg/ml). Concentrations were determined by amino acid analysis with the use of norleucine as an internal standard and spectrophotometrically (94,240 and 19,180 M^{-1} cm^{-1} for HLA-A2 and β_2M, respectively, at 280 nm). Ellipticities are expressed on a molar residue basis. Spectra were recorded with use of a 1-mm cell and an Aviv 62DS spectropolarimeter equipped with a thermoelectric temperature controller.
26. Reversibility of the unfolding transition was demonstrated by a series of independent experiments each including two heating cycles separated by cooling to 25°C. The first heating cycles were scanned from 25°C to various temperatures; such a cycle between 25° and 68°C is shown in Fig. 3C. The CD spectrum of unfolded protein at 68°C, recorded separately, is shown in Fig. 3B. After cooling immediately to 25°C, the CD spectrum recorded at equilibrium (2 hours) (Fig. 3B) is nearly identical to that of the native protein. A second heating cycle to 75°C (Fig. 3C) closely resembled the first cycle, another indication that cooling resulted in correctly renatured HLA-A2. If the sample was maintained at 68°C for short times (15 min) before cooling to 25°C, a decrease in the extent of reversibility was observed, indicating that kinetic factors are responsible for the formation of some irreversibly unfolded HLA-A2. When the first heating cycle was between 25° and 80°C, the longer time above 68°C appeared to be responsible for a slightly reduced reversibility.
27. Denaturation curves were fit by a nonlinear least squares analysis (Kaleidagraph, Synergy Software) to the following relation describing a two-state unfolding process

$$\theta(T) = \theta_u + [(\theta_f - \theta_u)/1 + \exp(x)]$$

$$x = (-\Delta H_m/R)(1/T - 1/T_m) + (\Delta C_p/R)[(T_m/T - 1) + \ln T/T_m]$$

where $\theta(T)$ is the observed residue ellipticity at T, and θ_f and θ_u are linear functions of temperature for the pre- and post-transition region, respectively. T_m is the midpoint temperature of the unfolding transition, ΔH_m is the enthalpy change at T_m, R is the gas constant, and ΔC_p is the difference in heat capacity between the folded and unfolded states. We obtained initial estimates for T_m and ΔH_m from the van't Hoff equation $\Delta H = RT^2(\delta \ln K/\delta T)$, using values of K, equilibrium constant, calculated in the narrow temperature range of the transition region from the relation $K = [\theta_f(T) - \theta(T)]/[\theta(T) - \theta_u(T)]$. The van't Hoff plots were fit to a second-order polynomial equation, and ΔH_m was calculated from the first derivative of the equation at $T = T_m$ and $\ln K = 0$. Values of ΔC_p were assumed to be independent of temperature [P. L. Privalov and S. J. Gill, *Adv. Protein Chem.* **39**, 191 (1988)] and were estimated from $\Delta C_p = (\delta \Delta H/\delta T)_p$ with values of ΔH calculated in the narrow temperature range of the transition region.
28. Leu fits better than Val into the binding pocket at position 2 and allows formation of shorter hydrogen bonds between peptide main chain atoms at position 2 and MHC side chains (*6*). When Val occupies the binding pocket at position 9, MHC residues Arg^{97} and Tyr^{116} orient to form favorable intramolecular hydrogen bonds, absent in the x-ray structure of the HLA-A2–WT complex (*6*).
29. M. H. Hecht, H. C. M. Nelson, R. T. Sauer, *Proc. Natl. Acad. Sci. U.S.A.* **80**, 2676 (1983); M. H. Hecht, J. M. Sturtevant, R. T. Sauer, *ibid.* **81**, 5685 (1984); R. L. Heinrikson, *Methods Enzymol.* **47**, 175 (1977).
30. Thermolysin digestions at different temperatures were carried out for 15 min (60 min for G1-Ndel) in 10 mM MOPS (pH 7.5) containing 2 mM $CaCl_2$ at an enzyme:substrate ratio of 1:300 (w/w). Incubations were terminated by addition of EDTA to a concentration of 10 mM and immediate cooling of samples on ice. Products were analyzed by SDS-PAGE (15%).
31. V. Cerundolo *et al.*, *Eur. J. Immunol.* **21**, 2069 (1991); S. Y. Sauma *et al.*, *Human Immunol.* **37**, 252 (1993).
32. T. Elliott, J. Elvin, V. Cerundolo, H. Allen, A. Townsend, *Eur. J. Immunol.* **22**, 2085 (1992); M. Matsumura, Y. Saito, M. R. Jackson, E. S. Song, P. A. Peterson, *J. Biol. Chem.* **267**, 23589 (1992).
33. F. Latron *et al.*, *Science* **257**, 964 (1992).
34. Peptides likely to extend out at the COOH-terminal binding site have been identified in peptide binding studies [Y. Chen *et al.*, *J. Immunol.* **152**, 2874 (1994); A. C. Olsen *et al.*, *Eur. J. Immunol.* **24**, 385 (1994)], and one example has been observed by x-ray crystallography [E. J. Collins, D. N. Garboczi, D. C. Wiley, unpublished results].
35. Peptides with one residue deleted at the NH_2-terminus have been reported [U. Utz, S. Koenig, J. E. Coligan, W. E. Biddison, *J. Immunol.* **149**, 214 (1992); (*19*)], and a peptide 8-mer too short to reach the NH_2-terminal binding site has been observed by x-ray crystallography to leave that site unoccupied [P. Ghosh and D. C. Wiley, unpublished results].
36. W. J. Becktel and J. A. Schellman, *Biopolymers* **26**, 1859 (1987).
37. Values for $\Delta\Delta G$, the difference in Gibb's free energy of unfolding between mutant and control complexes, were calculated at 60°C, a value intermediate among T_m values of HLA-A2 complexes, from the approximation $\Delta\Delta G = \Delta T_m \cdot \Delta S$ (*36*). Values of ΔT_m are equal to T_m (mutant) − T_m (control), where the control is L9A for G1-Ndel and A9-Cdel, and WT or I2L+L9V for I2A+L9A. Values for ΔS at 60°C for L9A, WT, and I2L+L9V are 0.209, 0.214, and 0.186 kcal/mol·*K*, respectively (*27*). An average value of ΔC_p = 3.6 kcal/mol·*K* obtained from nonlinear least squares analysis of denaturation curves (*27*) was used.
38. M. Carson, *J. Mol. Graphics* **5**, 103 (1987).
39. We thank D. Garboczi, F. Hughson, T. Jardetzky, D. Madden, and L. Stern for many helpful discussions; P. Bjorkman, D. Garboczi, F. Hughson, D. Madden, and L. Stern for critical reading of the manuscript; H.-C. Guo for preparing Fig. 1; D. Minor for help with CD analysis; and the Mass Spectrometry Facility of the Harvard University Chemistry Department. M.B. is supported by a Cancer Research Institute fellowship. D.C.W. is an Investigator of the Howard Hughes Medical Institute.

15 March 1994; accepted 27 May 1994

Fibrous Mini-Collagens in *Hydra* Nematocysts

T. W. Holstein,* M. Benoit, G. v. Herder, G. Wanner, C. N. David, H. E. Gaub*

Nematocysts (cnidocysts) are exocytotic organelles found in all cnidarians. Here, atomic force microscopy and field emission scanning electron microscopy reveal the structure of the nematocyst capsule wall. The outer wall consists of globular proteins of unknown function. The inner wall consists of bundles of collagen-like fibrils having a spacing of 50 to 100 nanometers and cross-striations at intervals of 32 nanometers. The fibrils consist of polymers of "mini-collagens," which are abundant in the nematocysts of *Hydra*. The distinct pattern of mini-collagen fibers in the inner wall can provide the tensile strength necessary to withstand the high osmotic pressure (15 megapascals) in the capsules.

Nematocysts are exocytotic organelles that are characteristic of the phylum Cnidaria. There are at least 25 morphologically different capsule types, which are involved in a variety of functions, including capture of prey, defense, and locomotion (*1*). Capsules have very high internal pressures of up to 15 MPa (*2*), which drive nematocysts' discharge, during which the capsule's internal tube is everted (*3*). High-speed cinematography has shown that the entire process takes about 3 ms and takes place at accelerations of up to 40,000*g* (*4*). The explosive discharge of nematocysts is thus one of the fastest events in biology. The extreme osmotic pressure in resting capsules and the extraordinary speed of

T. W. Holstein, Zoological Institute, J. W. Goethe Universität Frankfurt, 60590 Frankfurt am Main, Germany.
M. Benoit, G. v. Herder, C. N. David, Zoological Institute, Ludwig Maximilians Universität München, 80333 München, Germany.
G. Wanner, Botanical Institute, Ludwig Maximilians Universität München, 80638 München, Germany.
H. E. Gaub, Department of Physics, Technische Universität München, 85748 Garching, Germany.
*To whom correspondence should be addressed.

evagination lead one to expect high tensile strength in the capsule wall. By combining atomic force microscopy (AFM) and field emission scanning electron microscopy (FESEM) with biochemical methods, we resolved the structure of the capsule wall, and we show that the molecular basis for its high tensile strength resides in fibers of a form of collagen: "mini-collagen" (*5*).

The capsule wall consists of an outer layer (100 nm thick), which can be enzymatically dissociated with pronase B, and an inner layer (200 nm thick) composed of mini-collagen (*5*). The capsule itself, but not the tube, was covered with densely packed globular particles (50 to 100 nm in diameter) of uniform shape (Fig. 1, A and B) (*6*, *7*). Treatment of capsules with SDS or with the reducing agent dithiothreitol (DTT) (65 μM) at an alkaline pH removed this outer layer and revealed an underlying inner wall that appeared, by FESEM analysis (*7*), to have a smooth surface (Fig. 1C). The outer globular layer that was removed by DTT treatment was composed primarily of proteins larger than 40 kD (Fig. 1D) (*8*). The inner wall consisted primarily of small proteins, 12 to 16 kD and 25 to 40 kD in size (Fig. 1D), which were rich in proline and constituted mini-collagen monomers and covalently cross-linked dimers and trimers (*5*).

The mechanical stability of the inner wall may be estimated as follows: The tension in a spherical shell under internal pressure is given by

$$\sigma \text{ sphere} = (P \times r)\ (2d)^{-1}$$

If we assume an internal pressure P of 15 MPa (*2*), a radius r of 5 to 10 μm (*3*), and the thickness of the inner wall, d, to be 200 nm (*3*), the tension of the inner wall turns out to be σ = 190 to 375 MPa. In order to sustain this enormous tension, the tensile strength of the capsule must be nearly as high as that of steel.

Collagens can form either fibrils or net-like structures to withstand high loads (*9*). To distinguish between these potential structures in the capsule wall in vivo, we investigated the inner wall in more detail by AFM (*10*, *11*). Isolated nematocyst capsules from *Hydra vulgaris* polyps were mechanically immobilized on nucleopore filter membranes by being sucked partially into the pores (*12*). The nematocysts were imaged with an atomic force microscope equipped with a fluid cell (*13*). Using 5-μm-long carbon tips (*13*) and operating at imaging forces below 5 nN, we identified densely packed structures that were 60 to 180 nm apart (Fig. 2A). The apparent shape of these structures is also a function of the tip geometry, but on the basis of the spacing of the structures, they appear to be equivalent to the globular structures of the outer wall that were seen by FESEM.

In order to image the inner wall, we dissected the outer wall by passing the tip repeatedly over the capsule surface. After several sweeps with the tip, the layer of globular particles was completely removed, exposing the inner wall of the nematocyst capsule. This surface showed numerous, densely packed, fiber-like structures, spaced 50 to 100 nm apart (Fig. 2, B and C) and oriented at an angle of about 40° to the longitudinal axis of the capsule. Because the inner wall is about 200 nm thick (*3*), only two to four layers of mini-collagen fibers can fit into it. Similar fibers were found when the outer wall was removed chemically by DTT treatment (Fig. 2E). The surface corrugations were extremely shallow under those conditions and could be recorded only in the deflection mode, probably because the supramolecular organization was altered by DTT and fixation (this might also explain why FESEM failed to resolve fibers properly) (see Fig. 1C). When intact capsules were induced to discharge (*2*), we found similar fiber-like structures running along the twisted tubes (Fig. 2F), which suggests that the fibers of the capsule's inner wall continue along the tube. At the base of the capsule, the fibers

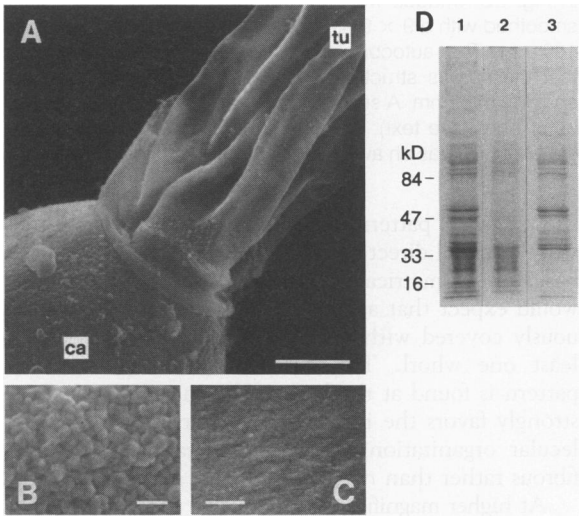

Fig. 1. Structure and biochemical dissection of a nematocyst capsule. (**A**) FESEM image of a discharged stenotele showing the rough capsular surface (ca) and the smooth surface of the everted tube (tu); scale bar, 1 μm. (**B**) FESEM image of the globular particles of the outer wall; scale bar, 100 nm. (**C**) Dithiothreitol treatment (65 μM) removes the outer layer, revealing a smooth underlying inner wall (FESEM image); scale bar, 200 nm. (**D**) SDS-PAGE analysis of DTT-treated capsules (65 μM) with the use of polyacrylamide gradient gels (4 to 20%) stained with Coomassie blue. Lane 1, control nematocysts [corresponds to (A)]; lane 2, pellet of DTT-treated capsules [corresponds to (C)]; lane 3, supernatant of DTT-treated capsules [corresponds to (B)].

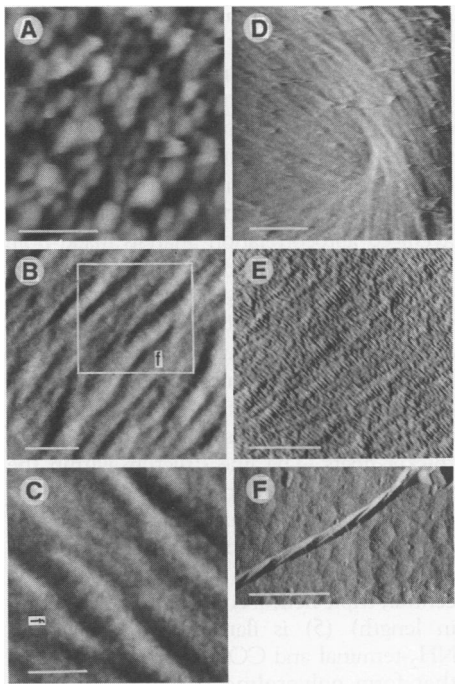

Fig. 2. AFM dissection of a nematocyst capsule. (**A**) AFM image of the outer wall, showing the globular surface (the microscope was in constant force mode at ~2.5 nN and had a scan speed of five lines per second); scale bar, 500 nm. (**B** through **D**) AFM images after the outer wall was physically removed by the cantilever tip (see text). (B) Fibers of the inner wall, oriented obliquely to the longitudinal axis of the capsule; scale bar, 200 nm. (C) Labeled area of (B), imaged with the same tip at a higher magnification and in a different scanning direction (tilted clockwise by 90°, as indicated by f) (note individual fibers showing a 30- to 40-nm periodicity); scale bar, 100 nm. (D) Whorl-like pattern of fibers at the base of a capsule; scale bar, 500 nm. (**E**) AFM image (made in deflection mode) of DTT-treated (65 μM) and chemically fixed capsules (2.5% glutaraldehyde in 50 μm of phosphate buffer), showing fibers with 30- to 40-nm periodicity; scale bar, 500 nm. (**F**) Low-magnification image of a discharged nematocyst tube; intact capsules were induced to discharge (*2*). Note the fibers and the twisted pattern of the everted tube; scale bar, 10 μm. For (B) through (D) and for (F), the microscope was in constant force mode at ~50 nN and had a scan speed of five lines per second. For (A) through (F), different capsule preparations and different tips were used; images are representative of over 100 imaged capsules, with 10 to 20 images made per capsule at different magnifications, scan directions, and imaging forces. Fifty independent preparations [see (*6*) and (*12*)] were done, most with a new tip (*13*).

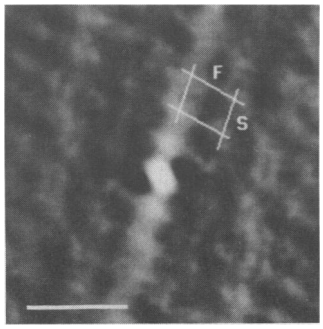

Fig. 3. Autocorrelation analysis of five independent images (from different capsule preparations, made with different tips) of an area shown in Fig. 2C. Images were added together and smoothed with a 9 × 9 hat operator; scale bar, 100 nm. The autocorrelation analysis shows that the fibrous structure (F) has an average spacing of 52 nm. A second ridge can be seen at 110 nm (see text). The fine structure within the fibers (S) has an average spacing of 32 nm.

show a whorl pattern, in which fibers converge from all directions (Fig. 2D). On the basis of geometrical considerations, one would expect that a sphere that is continuously covered with fibers would show at least one whorl. The fact that such a pattern is found at the base of the capsule strongly favors the idea that the supramolecular organization of the inner wall is fibrous rather than net-like.

At higher magnification, individual fibers show periodic cross-striations that consist of alternating grooves and ridges (Fig. 2C). Figure 2C shows the central area of Fig. 2B, but scanned in an orientation rotated 90° from that in Fig. 2B. Fibers have the same periodicity, and the rotation of the fiber orientation is in accordance with the rotation of the scanning direction. Small differences in details of fiber structure are due to the finite size of the tip or to minor distortions caused by the scanning process (or both). Figure 3 shows an averaged autocorrelation analysis made from images that were recorded from the area shown in Fig. 2C. The autocorrelation analysis shows that the fibrous structure that is clearly visible in Fig. 2C has an average spacing of 52 nm. A further peak at 110 nm could be due either to the second order of the autocorrelation analysis or to a second class of thicker fibers. The fine structure within the fibers has an average spacing of 32 nm.

The structural model of mini-collagens (*5*) suggests that these molecules can form rod-shaped structures that are 50 nm long. The central, triple helical collagen domain (15 nm in length) (*5*) is flanked by cysteine-rich NH_2-terminal and COOH-terminal domains that form polyproline II helices (9 to 26 nm in length). The fibers in the inner wall could thus consist of mini-collagen polymers in which the NH_2- and COOH-terminal domains overlap and are stabilized by S–S bridges (Fig. 4). Such protofilaments would have a characteristic surface profile in which triple helical domains (4 nm in diameter) alternate with polyproline II helices (8 nm in diameter). In such a fiber, the repeating pattern from one triple helical domain to the next can vary between 20 and 40 nm, which is highly consistent with the distinct periodicity shown by AFM (Fig. 3). Our observations support a model (Fig. 4) in which the tensile strength of the capsule is created by layers of mini-collagen fibers, which begin at the base and spread up and around the capsule. The fibers in the different layers are oriented at an angle to each other (Fig. 2), so that an amphora is formed that has high tensile strength in all directions. Such a model is also compatible with the pathway of capsule morphogenesis in which polymerization of the wall begins at the capsule base and progresses toward the tube (*14*).

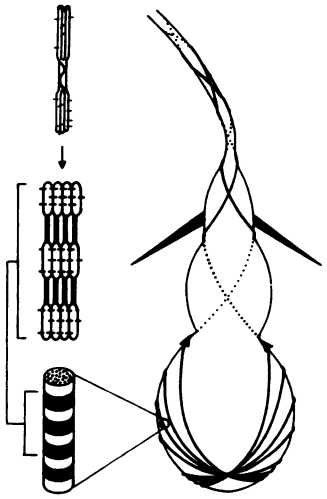

Fig. 4. Model of the supramolecular organization of a nematocyst capsule's inner wall. Mini-collagen molecules have a central triple helical domain (12 to 14 nm in length) flanked by cysteine-rich polyproline II helices (9 to 22 nm in length). Polymer formation occurs by S–S linkage of overlapping NH_2- and COOH-terminal domains, which yields a repeating pattern of triple helical (solid lines) and cysteine-rich (open bars) domains (S–S bridges are indicated by lateral branches). Some of the fibrils of the inner wall extend distally to form the wall of the tube.

Nematocyst capsules appeared early in evolution, probably developing from simpler extrusive organelles such as those found in several classes of protozoa (*15*). The high osmotic pressure required for the exocytotic discharge of these organelles (*16*) may have been an important constraint on the evolution of collagen molecules.

REFERENCES AND NOTES

1. R. N. Mariscal, in *Coelenterate Biology*, L. Muscatine and H. M. Lenhoff, Eds. (Academic Press, New York, 1974), pp. 129–178.
2. J. Weber, *Eur. J. Biochem.* **184**, 465 (1989).
3. P. Tardent and T. W. Holstein, *Cell Tissue Res.* **224**, 269 (1982).
4. T. W. Holstein and P. Tardent, *Science* **223**, 830 (1984).
5. E. M. Kurz, T. W. Holstein, B. M. Petri, J. Engel, C. N. David, *J. Cell Biol.* **115**, 1159 (1991).
6. We used polyps of *Hydra vulgaris* [T. W. Holstein, P. Tardent, R. D. Campbell, *Nature* **346**, 21 (1991)] and isolated pure capsules by centrifugation of tissue homogenates through 50% Percoll gradients according to the method of Weber [J. Weber, M. Klug, P. Tardent, *Comp. Biochem. Physiol.* **88B**, 855 (1987)]. Under these conditions, capsules form a pellet that is free of other cellular components. We used 1 ml of tissue homogenate from 1000 animals and obtained 3 × 10^7 capsules, which were stored in aliquots at −80°C. For the experiments reported here, 15 capsule isolations were done.
7. Isolated cysts were fixed in 2.5% glutaraldehyde solution containing 50 μM phosphate buffer, which was also used for the post-fixation in 2% OsO_2. A graded series of acetone concentrations was used for dehydration. Critically point-dried specimens were mounted on arsine-dotted silicon crystal wafers with the use of TEMPFIX (Plano W. Plannet, Marburg, Germany) at room temperature; thereafter, they were sputtered with a layer ≈20 to 30 Å thick of gold-palladium alloy by means of a neutral particle gun (Anton Paar, Graz, Austria). We used a HITACHI S-800 field emission scanning microscope.
8. SDS–polyacrylamide gel electrophoresis (PAGE) of solubilized nematocyst proteins was done according to standard protocols on gradient gels (4 to 20%) with the use of the Laemmli buffer system.
9. S. A. Wainwright, W. D. Biggs, J. D. Currey, J. M. Gosline, *Mechanical Design in Organisms* (Arnold, London, 1976); R. Mayne and R. E. Burgeson, Eds., *Structure and Function of Collagen Types* (Academic Press, New York, 1987); R. E. Burgeson, *Annu. Rev. Cell Biol.* **4**, 551 (1988).
10. G. Binnig, C. F. Quate, C. Gerber, *Phys. Rev. Lett.* **56**, 930 (1986); B. Drake *et al.*, *Science* **243**, 1586 (1989); A. L. Weisenhorn *et al.*, *Biophys. J.* **58**, 1251 (1990); M. Radmacher, R. W. Tillmann, M. Fritz, H. E. Gaub, *Science* **257**, 1900 (1992); M. Radmacher, R. W. Tillmann, H. E. Gaub, *Biophys. J.* **64**, 735 (1993).
11. H. G. Hansma and J. Hoh, *Annu. Rev. Biophys. Biomol. Struct.* **23**, 115 (1994); E. Henderson, P. G. Haydon, D. S. Sakaguchi, *Science* **257**, 1944 (1992); W. Häberle, J. K. H. Hörber, F. Ohnesorge, D. P. E. Smith, G. Binnig, *Ultramicroscopy* **42**, 1161 (1992); A. Engel, *Annu. Rev. Biophys. Biophys. Chem.* **20**, 79 (1991).
12. Intact nematocysts were purified (*6*) and mounted on COSTAR nucleopore filter membranes (Costar, Cambridge, MA) (pore sizes, 5 to 12 μm) by suction of a capsule suspension (10^7 capsules per milliliter) through the filters. Adhesion of intact capsules to the filters was greatly improved by the following treatment: Nucleopore filters were coated with gelatin (2%), then treated with glutaraldehyde (4%), and finally washed with distilled water. A total of 43 filter preparations were analyzed by AFM.
13. We used a Nanoscope III atomic force microscope from Digital Instruments. The carbon tips were grown onto conventional silicon-nitride cantilevers (Digital Instruments) with the help of A. Engel's group (Biozentrum, Basel, Switzerland), following the procedure given in D. Keller and C. Chih-Chiung, *Surfactant Sci. Ser.* **268**, 333 (1992).
14. T. W. Holstein, *J. Ultrastruct. Res.* **75**, 276 (1981).
15. K. Hausmann, *Int. Rev. Cytol.* **56**, 197 (1978).
16. A. Finkelstein, J. Zimmerberg, F. S. Cohen, *Annu. Rev. Physiol.* **48**, 163 (1986); R. W. Holz, *ibid.*, p. 175.
17. Supported by the Deutsche Forschungsgemeinschaft (C.N.D., H.E.G., and T.W.H.). Technical support from Digital Instruments Corporation and helpful discussions with M. Fritz and H. MacWilliams are gratefully acknowledged. We thank B. Schreck and T. Nüchter for providing the preparations for Fig. 2E.

31 January 1994; accepted 23 May 1994